Supporting Information

Source-specific health risk analysis on particulate trace elements: Coal combustion and traffic emission as major contributors in wintertime Beijing

Ru-Jin Huang[*,†], Rui Cheng[†], Miao Jing[‡], Lu Yang[†], Yongjie Li[‖], Qi Chen[§], Yang Chen[⊥], Jin Yan[†], Chunshui Lin[†,¶], Yunfei Wu[▽], Renjian Zhang[▽], Imad El Haddad[#], Andre S. H. Prevot[#], Colin D. O'Dowd[¶], Junji Cao[†]

[†]Key Laboratory of Aerosol Chemistry and Physics, State Key Laboratory of Loess and Quaternary Geology, Institute of Earth and Environment, Chinese Academy of Sciences, Xi'an 710061, China

[‡]COE lab of Thermofisher Scientific Technology, Shanghai 201206, China

[‖]Department of Civil and Environmental Engineering, Faculty of Science and Technology, University of Macau, Taipa 000000, Macau

[§]State Key Joint Laboratory of Environmental Simulation and Pollution Control, College of Environmental Sciences and Engineering, Peking University, Beijing 100871, China

[⊥]Chongqing Institute of Green and Intelligent Technology, Chinese Academy of Sciences, Chongqing 400714, China

[¶]School of Physics and Centre for Climate and Air Pollution Studies, Ryan Institute, National University of Ireland Galway, University Road, Galway H91CF50, Ireland

[▽]RCE-TEA, Institute of Atmospheric Physics, Chinese Academy of Sciences, Beijing 100029, China

[#]Laboratory of Atmospheric Chemistry, Paul Scherrer Institute (PSI), 5232 Villigen, Switzerland

*corresponding authors, email: rujin.huang@ieecas.cn

The Supporting Information contains:
Number of figures: 6 (Figure S1-S6)
Number of tables: 7 (Table S1-S7)
Number of pages: 16

Sampling site description

The sampling site was in the Institute of Atmospheric Physics, Chinese Academy of Sciences, located between the third and fourth ring roads in the northwest Beijing. It is within a combination district of education, commercial, and residential units, a typical urban location in Beijing.

Reagents and standard reference materials

Milli-Q water (18.2 MΩ cm^{-1}; Millipore, Massachusetts, USA) was used for preparation of reagents and standards. Analytical grade reagents of HNO_3 (JT Baker, Chemical Co., Phillipsburg, NJ, USA), $HONH_3Cl$ (98.0%, Sigma-Aldrich, USA), CH_3COOH (Sigma-Aldrich), CH_3COONH_4 (Sigma-Aldrich), perchloric acid solution (1.0 M, Sigma-Aldrich), H_2O_2 (30 wt.% in H_2O, Aladdin, Shanghai, China), and HF (40 wt.% in H_2O, J&K., Beijing, China) were used for extraction and digestion. The multi-element standards ([7697-37-2], in HNO_3, 20 μg mL^{-1}, SPEX CertiPrep, Avenue, Metuchen, USA) were obtained from Inorganic Venture for instrumental calibration of Inductively coupled plasma mass spectrometry (ICP-MS). The standard GBW07406 (GSS-6) used for recovery analysis and quality control was purchased from the National Research Center for Geoanalysis, China.

Sequential extraction procedure

A punch of filter (47 mm diameter) was used for each sample. Half of the punch was used for the sequential extraction and the other half for total digestion. After each extraction step (see Table S1), the extract was separated from the residues by centrifuging the mixture at 4500 rpm for 15 min. The supernatant was carefully transferred to a Teflon beaker. The residual filter was rinsed with fresh extraction solution and then centrifuged again, and finally the supernatant was decanted into the same Teflon beaker. The combined supernatants were heated and purged to 1-2 mL, then diluted into 5 mL with 2% HNO_3. The extract was then filtered through a 0.22 μm PTFE syringe filter (Sterlitech Corp., Kent, WA, USA) and stored at 4 °C until ICP-MS analysis.

We used a four-step extraction procedure for the chemical fractionation of trace elements in $PM_{2.5}$. In the fourth step, quartz filter can digest in the reagent mixture of HNO_3+H_2O_2+HF to give high extraction efficiency for the 'residual fraction' of trace elements, while Teflon filter cannot digest leading to potential underestimate. We also tested the extraction efficiencies using the same extraction procedure on Quartz and Teflon filter samples taken simultaneously. Our results show that extraction efficiencies of Teflon filter samples were only about 50% of that of quartz filter samples. A number of previous studies also used quartz filters for metal analysis in PM.[1,2] As for the background issue, the data reported in this study were corrected for the values from blank samples. Those elements of high background concentrations in quartz filters (e.g., K, Na, Mg, Al, Ca) were not discussed in our study.

Quality assurance / quality control

The recovery of certified materials

The certified material (GSS-6) was used to assess the accuracy of this method. The recoveries for total concentrations of the fourteen elements ranged from 81% to 112%, supporting that the extraction and measurement methods, as part of the quality control/quality assurance

protocol, were sufficient and effective. The detailed results of recoveries are listed in Table S2.

Internal check of the recovery of this method

Internal extraction efficiency of the sequential extraction was examined by comparing the sum of the concentration extracted in each fraction (i.e., F1, F2, F3, and F4) with the total concentration (TC) measured in the digested solution for each element. The recoveries ranged from 78% to 123% for these 14 elements, demonstrating the high extraction efficiency and reliability of this method (see Table S3).

ICP-MS analysis

The ICP-MS (iCAP Q, ThermoFisher Scientific, Waltham, MA, USA) was optimized daily. A seven-point calibration curve (i.e., 1, 2, 5, 10, 20, 50, 100 μg L^{-1}) was established for each targeted element, and the regression coefficients for all elements were >0.999. For the analysis, ^{103}Rh and ^{185}Re were added as internal standards at a concentration of 10 μg L^{-1} in 2% HNO_3. A spiked sample was analyzed for every 10 samples. Blank filter samples were extracted and analyzed following the same procedures. All data reported here were corrected for the field blanks. The accuracy was estimated by analyzing the reference material GBW07406 (GSS-6). The differences between the measured and certified values ranged from -19% to 12% for the fourteen elements, demonstrating a good accuracy of the method.

PMF analysis

The EPA PMF is one of the receptor models that the US EPA's Office of Research and Development has developed. PMF was used to identify and quantify the main sources of these elements. The PMF receptor model has been widely used for $PM_{2.5}$ source apportionment. In this study, the concentrations and uncertainties of fourteen trace elements were included in the PMF 5.0. If the concentration is less than or equal to the method detection limit (MDL) provided, the uncertainty (Unc) is calculated using the following equation [3,4]

$$\mathrm{Unc}=\frac{5}{6}\times MDL \quad (1)$$

If the concentration is greater than the *MDL*, the uncertainty is then calculated as the detection limits (MDL) and a relative error (5%) summed in quadrature,

$$\mathrm{Unc}=\sqrt{(Error\ Fraction\ \times\ concentration)^2+(MDL)^2} \quad (2)$$

The model is a multivariate factor analysis and descriptive model, providing a solution that minimizes an objective function *Q* based on uncertainty of each measurement. In this study, the PMF solutions from 3 to 6 factors were examined, and the 4-factor solution is selected as it provides the most interpretable profiles and minimal *Q* value. In Figure S4 we show the correlation (R^2) of each element with each source identified by PMF. From the figure, we can see that relatively high correlation coefficients are obtained between the source markers and a specific source. For example, coal combustion is closely correlated with As (R^2=0.83), Cd (R^2=0.91) and Pb (R^2=0.87). Traffic-related emission is highly correlated with Ni (R^2=0.90) and Ba (R^2=0.90). Oil combustion shows a high R^2 value with V (0.86) and dust source is

highly correlated with Ti (0.96) and Fe (0.81). Figure S5a, b and c show the source profiles resolved from the PMF model with 3, 5 and 6 factors, respectively. In the 3-factor solution (Figure S5a), factors 1 and 3 are likely traffic-related emission and coal combustion, respectively. However, factor 2 is a mixture of multiple sources, explaining a major fraction of the variability of both Ti and V, which typically arise from distinct sources: crustal material and oil combustion, respectively. The 4-factor solution enabled the separation of these two sources. In the 5-factor solution (Figure S5b), factor 2, factor 3 and factor 5 could be identified as dust, oil combustion and coal combustion, respectively. However, factor 1 and factor 4 seem to be a split from traffic-related emissions, potentially related to different, but unknown processes. Similar to the 5-factor solution, in the 6-factor solution (Figure S5c), coal combustion was split into factor 4 and factor 6 while traffic-related emission was split into factor 2 and factor 5. Therefore, the 4-factor solution was chosen as the optimal representation of our dataset. Figure S5d shows the value of goodness-of-fit parameter *Q* corresponding to the solution of different number of factors. It indicates that as the number of factors increases from 3 to 6, the Q/Q_{exp} value decreases. Considering the source profiles resolved from PMF analysis and the Q/Q_{exp} values, we chose the 4-factor solution.

Health risk assessment

According to the study by Volckens and Leith, the deposition efficiency of particles of size *i* that penetrate into the lung can be calculated as follows:[5]

$$Ei = -0.081+0.23\cdot \ln(d_p)^2 +0.23\cdot \sqrt{d_p} \quad (3)$$

Ei is the deposition fraction of particles of size *i* that penetrate into the lung, which is a complicated function of several deposition mechanisms that include impaction, interception, sedimentation, diffusion, and electric force. In this interpolation equation *Ei* depends on the aerodynamic particle diameter (*dp*) and can be used to estimate deposition to the lungs for particles between 0.01 and 10 μm in diameter.[5]

The winter days from 1 Nov 2013 to 31 Jan 2014 in Beijing were classified into three periods according to the $PM_{2.5}$ concentrations: low pollution days (≤ 75 μg m^{-3}, 49 days), moderate pollution days (75-170 μg m^{-3}, 30 days), and severe pollution days (≥ 170 μg m^{-3}, 13 days). The average concentrations of bioavailable fraction (exchangeable fraction (F1) and reducible fraction (F2)) of particulate-bound trace elements were used for calculation of exposure-point concentration (C). The exposure-point concentration (C) of individual elements in winter 2014 in Beijing was calculated following Eq. (4),

$$C = \frac{(F1+F2)_{clean}\times 49 + (F1+F2)_{moderate}\times 30 + (F1+F2)_{severe}\times 13}{90} \quad (4)$$

where the values of F1 and F2 are the average concentrations in exchangeable fraction and reducible fraction for each measured element during low, moderate and severe pollution days from 1st to 25th January 2014, respectively.

The carcinogenic and non-carcinogenic risks by airborne metals via direct inhalation of $PM_{2.5}$ were calculated using US Environmental Protection Agency (US EPA) human health risk assessment models (US EPA 2009),[6] which mainly involve exposure assessment and risk characterization. The methodology has been used in previous studies.[1,2]

Sensitive local residents were divided into two groups (i.e., children and adults). The

inhalation exposure concentration (EC), hazard quotient (HQ) for non-cancer risk, and carcinogenic risks (CR) by a toxic element in $PM_{2.5}$ were calculated following Eqs. (5-7)

$$EC = \frac{C \times Ei \times ET \times EF \times ED}{ATn} \quad (5)$$

$$HQ = \frac{EC}{RfC \times 1000\ \mu g\ mg^{-1}} \quad (6)$$

$$CR = IUR \times EC \quad (7)$$

where ET is the exposure time (24 h/day), EF is the exposure frequency (180 day/year), ED is the exposure duration (6 years for children and 24 years for adults), ATn is the averaging time (for non-carcinogens ATn = ED × 365 day/year × 24 h/day, and for carcinogens ATn = 70 year × 365 day/year × 24 h/day), RfC is the inhalation reference concentration (mg m^{-3}) and IUR is the inhalation unit risk (μg $m^{-3})^{-1}$). The RfC, IUR and default values for exposure were obtained from the user's guide and technical background document for the U.S. EPA region 9 regional screening level tables (US EPA, 2013).[7] Elements that induce non-carcinogenic but toxic effects are As, Cd, Co, Cr (VI), Mn, Ni and V. The RfC is used for the non-carcinogenic risk characterization. Elements that induce carcinogenic effects include As, Cd, Cr (VI), Ni, Co, and Pb. The IUR is used for the carcinogenic risk characterization.

The carcinogenic risk (CR) is the probability of an individual developing any type of cancer from lifetime exposure to carcinogenic hazards; the acceptable risk range is 1.0×10^{-6} according to the US EPA risk management guidelines (2009).[6] The sum of hazard quotient (HQ) below the precautionary level of 1 suggests that there is no significant risk of non-carcinogenic effects, while their values above 1 indicate that there is a chance of non-carcinogenic effects occurring, with a probability that tends to increase as the value of HQ increases (US EPA 2013).[7]

The carcinogenic and non-carcinogenic health risks of the four emission sources (oil combustion, dust, traffic-related and coal combustion) were assessed. The sum of carcinogenic risk (CR) of carcinogenic elements is used to assess the total carcinogenic risk of each emission source. For non-carcinogenic risks, the sum of hazard quotient (HQ) of non-carcinogenic elements is used to assess the overall non-carcinogenic effects of emission source.[1,2] The carcinogenic risk and non-carcinogenic risk of each source (CR_s and HQ_s) is calculated using Eqs. (8) and (9), respectively,

$$CR_s = \sum (CR_i \times RC_i) \quad \text{(i= As, Cd, Cr (VI), Ni, Co, and Pb)} \quad (8)$$

$$HQ_s = \sum (HQ_i \times RC_i) \quad \text{(i= As, Cd, Co, Cr (VI), Mn, Ni and V)} \quad (9)$$

RC_i is the relative contribution of emission source to individual elements resolved from source profiles (Figure S3).

The fraction ($F_{car(s)}$) of CR_s of each source in the total carcinogenic risk is calculated using Eq. (10), while the fraction ($F_{non(s)}$) of HQ_s of each source in the total non-carcinogenic risk is calculated using Eq. (11),

$$F_{car(s)} = \frac{CR_s \times RC_s}{\sum (CR_s \times RC_s)} \quad \text{(S= oil combustion, dust, traffic-related and coal combustion)} \quad (10)$$

192 $$F_{non(s)} = \frac{HQ_s \times RC_s}{\sum (HQ_s \times RC_s)}$$ (S= oil combustion, dust, traffic-related and coal combustion) (11)

193 RC_s is contribution of each emission source to total mass of measured elements in source
194 apportionment (Figure 3a in main text).
195 According to the guideline provided by U.S. EPA, Cr (VI) and Cr (III) are classified as Group
196 A (human carcinogens) and Group D (not classifiable for human carcinogenicity),
197 respectively. However, the total concentrations of Cr were obtained by the sequential
198 extraction method in this study. As the concentration ratio of Cr (VI) to Cr (III) in the
199 atmosphere was reported to be about 1:6, the concentration of Cr (VI) was approximated to be
200 one seventh of the total Cr concentration for the carcinogenic risk calculation.[8,9]
201

202 **Table S1**. Chemical fractions, reagents and operational conditions during the sequential
203 extraction procedure in this study.

Metal fraction	Reagent	Experimental conditions
Fraction 1. Soluble and exchangeable metals	15 mL Milli-Q water (pH=7.4)	agitation on a shaker at room temperature for 3 hours
Fraction 2. Carbonates, oxides and reducible metals	10 mL 0.25 M NH_2OH HCl at pH=2.0	agitation on a shaker at room temperature for 5 hours
Fraction 3. Bound to organic matter, oxidisable and sulphidic metals	7.5 mL H_2O_2 30 % + 7.5 mL H_2O_2 30% + 15 mL 2.5 M NH_4AcO at pH=3.0	agitation on a shaker at 95 ºC until near dryness + agitation on a shaker at 95 ºC until near dryness + agitation on a shaker at room temperature for 90 min
Fraction 4. Residual metals	4 mL HNO_3 + 2 mL H_2O_2 + 0.2 mL HF	10 min, 500 W, 130 ºC; 5 min, 500 W, 150 ºC; 5 min, 500 W, 180 ºC; 15 min, 500 W, 200 ºC

204 **Table S2**. The recovery of each element measured in standard sample GBW07406 (GSS-6)
205 following the same extraction procedure.

µg L^{-1}	Certified value	Measured value	Recovery %
Ti	1756.0	1615.5	92.5
V	52.0	45.8	88.1
Cr	30.0	31.5	105.3
Mn	580.0	551.0	95.9
Fe	24400.0	23668.0	97.8
Co	3.0	3.2	104.9
Ni	21.2	22.5	106.7
Cu	156.0	142.0	91.7
Zn	38.8	40.0	103.4
As	88.0	75.7	86.3
Sr	15.6	12.6	81.9
Cd	0.15	0.06	112.1
Ba	47.2	51.0	108.8
Pb	125.6	113.0	90.8

206

207

208

Table S3. The internal recovery of each element measured in $PM_{2.5}$ samples using the same extraction procedure.

Element	Average Internal Recovery %
Ti	78.4 ± 12.8
V	81.4 ± 13.4
Cr	123.3 ± 19.0
Mn	93.5 ± 15.0
Fe	85.1 ± 14.5
Co	77.5 ± 8.7
Ni	101.3 ± 9.7
Cu	92.8 ± 9.3
Zn	120.0 ± 27.7
As	84.4 ± 14.7
Sr	80.3 ± 11.7
Cd	101.1 ± 26.2
Ba	104.3 ± 9.5
Pb	120.3 ± 14.6

Table S4. The concentrations of trace elements during low pollution days, moderate pollution days, severe pollution days and entire sampling period. These abbreviations, such as L, M and S represent the concentrations of particulate-bound trace elements in low pollution days, moderate pollution days and severe pollution days, respectively.

ng m^{-3}	Low	Moderate	Severe	Full period	M/L	S/L
Ti	51.6 ± 14.7	59.0 ± 5.8	66.6 ± 20.4	56.6 ± 13.4	1.14	1.3
V	2.2 ± 0.7	4.7 ± 1.6	5.4 ± 2.0	3.7 ± 2.0	2.1	2.5
Cr	12.5 ± 3.1	17.1 ± 4.3	20.3 ± 1.2	15.4 ± 5.1	1.4	1.6
Mn	22.6 ± 6. 6	46.1 ± 13.1	77.8 ± 21.1	40.9 ± 22.1	2.0	3.4
Fe	536.7 ± 146.8	946.1 ± 315.3	1080.3 ± 322.6	771.8 ± 297.7	1.8	2.0
Co	0.6 ± 0.1	0.9 ± 0.2	1.3 ± 0.4	0.8 ± 0.3	1.5	2.2
Ni	52.6 ± 16.6	59.2 ± 17.4	67.4 ± 9.4	57.8 ± 17.6	1.1	1.3
Cu	35.2 ± 6.4	59.1 ± 10.6	77.4 ± 20.6	53.5 ± 19.5	1.7	2.2
Zn	73.9 ± 19.6	188.4 ± 68.4	427.9 ± 73.1	183.6 ± 138.0	2.5	5.8
As	4.5 ± 1.1	9.5 ± 2.8	32. 9 ± 13.0	11.0 ± 9.4	2.1	7.3
Sr	14.0 ± 4.3	17.6 ± 7.4	20.4 ± 8.0	16.4 ± 6.9	1.3	1.5
Cd	0.8 ± 0.3	2.0 ± 0.8	5.6 ± 2.3	2.0 ± 1.3	2.5	7.0
Ba	87.8 ± 25.2	119.8 ± 23.0	129.1 ± 29.3	109.4 ± 27.6	1.4	1.5
Pb	65.3 ± 20.1	147.8 ± 46.9	284.8 ± 94.4	138.1 ± 69.9	2.3	4.4

Table S5. The calculated EC, RfC and IUR.

Element	Concentration (ng m^{-3})	Exposure concentration (ng m^{-3})		RFC (mg m^{-3})	IUR $(\mu g\ m^{-3})^{-1}$
		Children	Adults		
As (Inorganic)	7.53E+00	2.61E+00	2.61E+00	1.50E-05	
Cd (Diet / water)	1.87E+00	6.48E-01	6.48E-01	1.00E-05	
Co	5.01E-01	1.74E-01	1.74E-01	6.00E-06	
Cr (VI)	4.84E-01	1.68E-01	1.68E-01	1.00E-04	
Mn (Diet)	3.10E+01	1.08E+01	1.08E+01	5.00E-05	
Ni (refinery dust)	2.60E+01	9.03E+00	9.03E+00	1.40E-05	
V	2.39E+00	8.30E-01	8.30E-01	1.00E-04	
As (Inorganic)	7.53E+00	2.24E-01	8.96E-01		4.30E-03
Cd (Diet / water)	1.87E+00	5.55E-02	2.22E-01		1.80E-03
Co	5.01E-01	1.49E-02	5.96E-02		9.00E-03
Cr (VI)	4.84E-01	1.44E-02	5.76E-02		8.40E-02
Ni (refinery dust)	2.60E+01	7.74E-01	3.10E+00		2.40E-04
Pb (acetate)	1.06E+02	3.16E+00	1.26E+01		8.00E-05

Table S6. Carcinogenic and non-carcinogenic risks resulted from trace elements via inhalation exposure to $PM_{2.5}$ in winter 2014 in Beijing.

Metal	Carcinogenic (CR)		Non-Carcinogenic (HQ)	
	Children	Adults	Children	Adults
As (Inorganic)	9.64E-07	3.85E-06	1.74E-01	1.74E-01
Cd (Diet / water)	9.99E-08	4.00E-07	6.48E-02	6.48E-02
Co	1.34E-07	5.37E-07	2.90E-02	2.90E-02
Cr (VI)	1.21E-06	4.84E-06	1.68E-03	1.68E-03
Mn (Diet)			2.15E-01	2.15E-01
Ni (refinery dust)	1.86E-07	7.43E-07	6.45E-01	6.45E-01
V			8.30E-03	8.30E-03
Pb (acetate)	2.53E-07	1.01E-06		

Sum	2.85E-06	1.14E-05	1.14E+00	1.14E+00

220 **Table S7**. Carcinogenic and non-carcinogenic risks resulted from four emission sources via
221 inhalation exposure to $PM_{2.5}$ in winter 2014 in Beijing.

Sources	Carcinogenic (CR)		Non-Carcinogenic (HQ)	
	Children	Adults	Children	Adults
Oil combustion	4.55E-08	1.82E-07	6.52E-02	6.52E-02
Traffic-related	1.21E-06	4.84E-06	6.89E-01	6.89E-01
Coal combustion	1.33E-06	5.31E-06	3.29E-01	3.29E-01
Dust	2.62E-07	1.05E-06	5.48E-02	5.48E-02

222

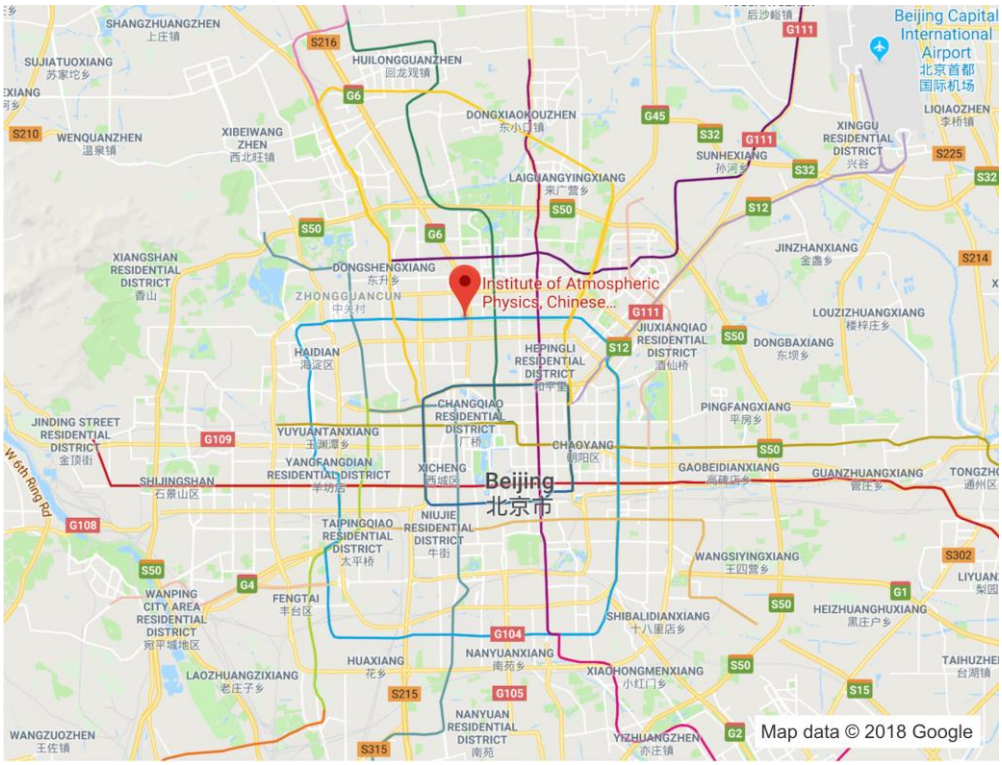

Figure S1. The sampling site in Beijing (http://www.google.com).

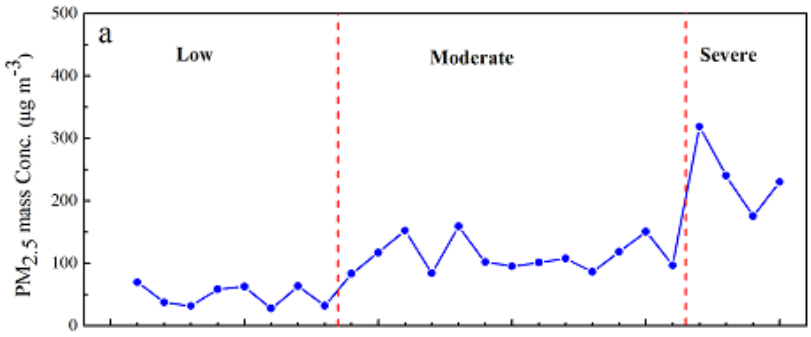

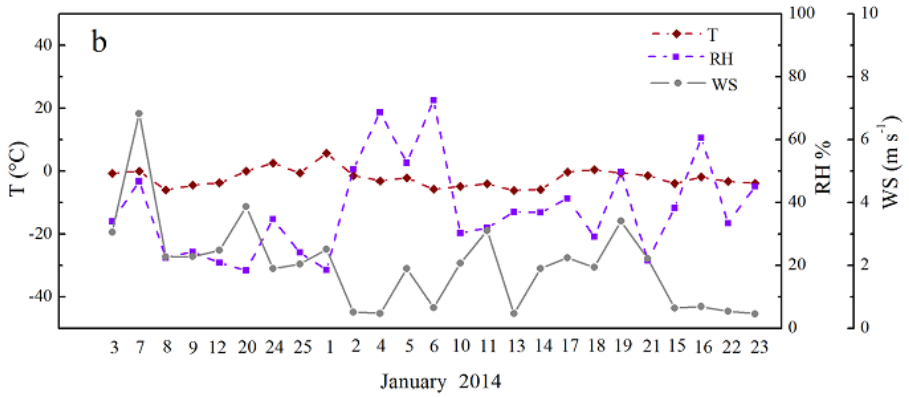

Figure S2. Daily $PM_{2.5}$ mass concentrations (a) and meteorological data (b) (T = temperature, RH = relative humidity and WS = wind speed) during the sampling period.

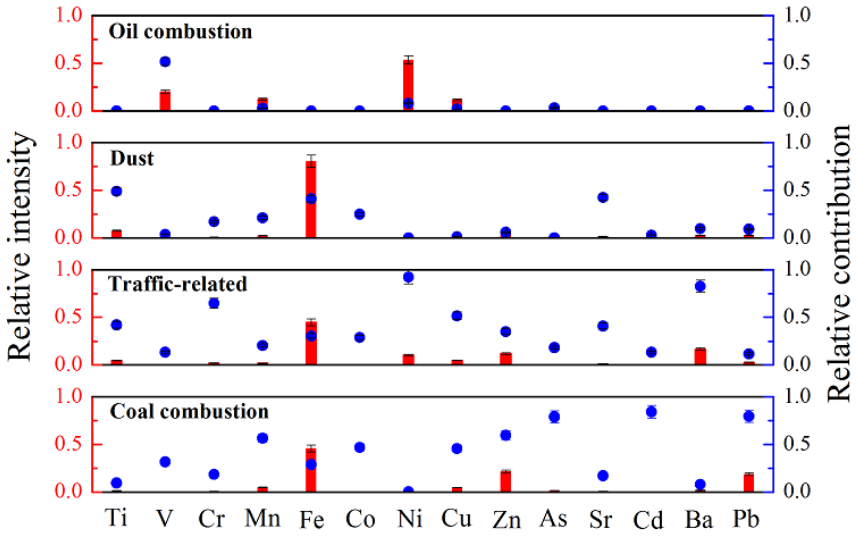

Figure S3. Source profiles resolved from the PMF model. The bars (left y axis) represent the relative intensity of element to each factor in ng m^{-3}, circles (right y axis) represent the fraction of the total predicted concentration for a given element.

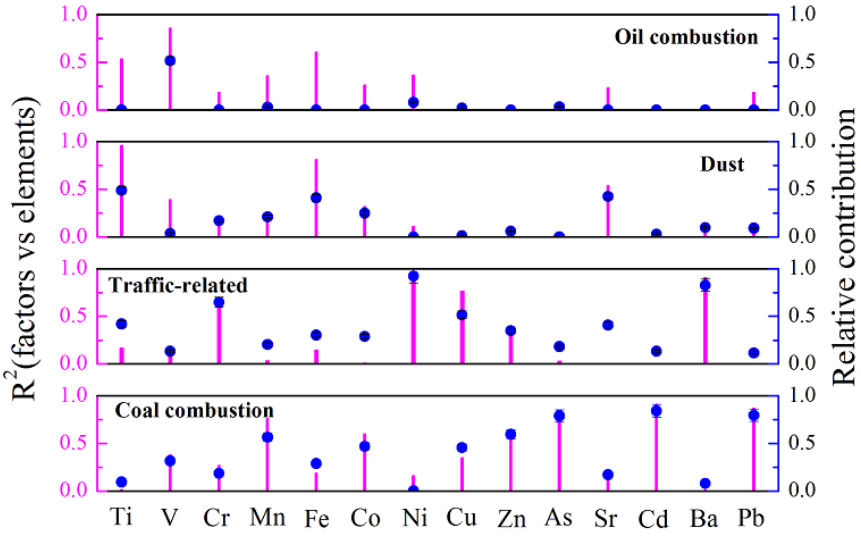

Figure S4. The correlations of each element with each source identified by the PMF model. The bars (left y axis) represent the R^2 (factors vs elements), while circles (right y axis) represent the contribution of the total predicted concentration for a given element

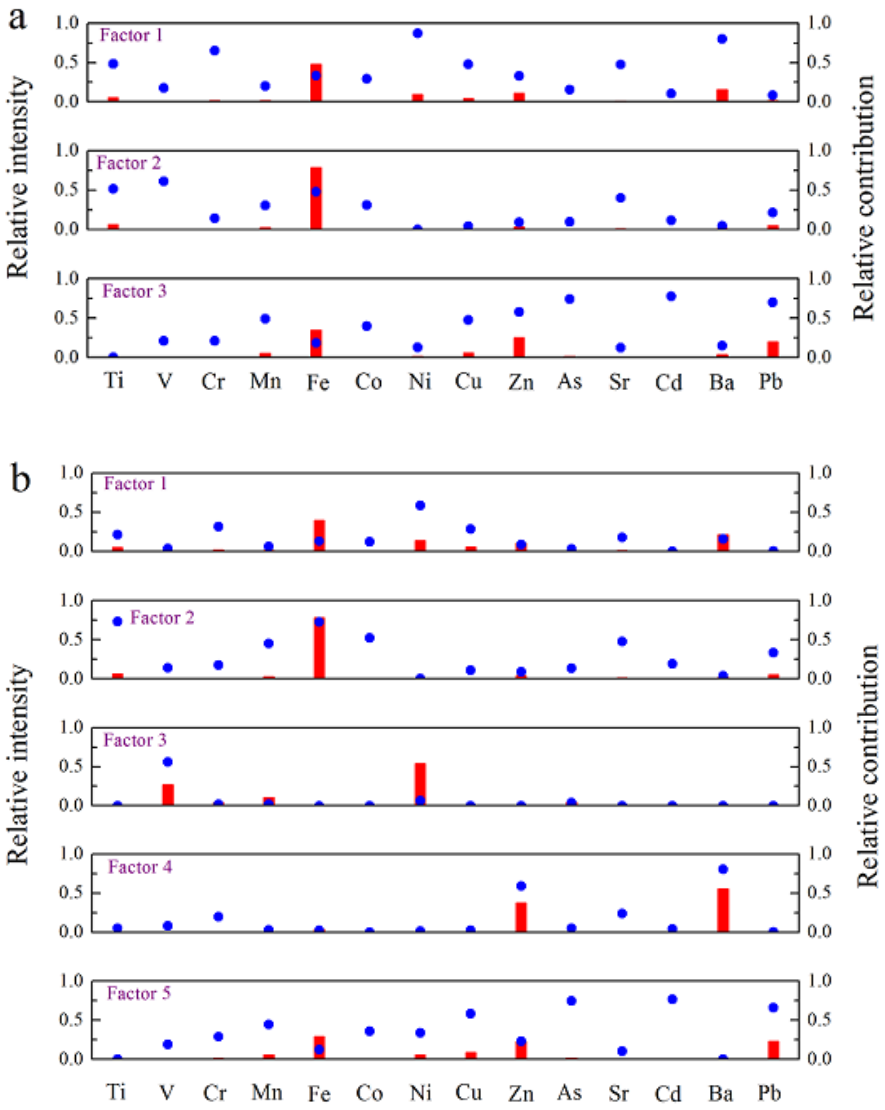
a
Factor 1
Factor 2
Factor 3
Relative intensity
Relative contribution
1.0
0.5
0.0
Ti V Cr Mn Fe Co Ni Cu Zn As Sr Cd Ba Pb
b
Factor 1
Factor 2
Factor 3
Factor 4
Factor 5
Relative intensity
Relative contribution
1.0
0.5
0.0
Ti V Cr Mn Fe Co Ni Cu Zn As Sr Cd Ba Pb

238

239

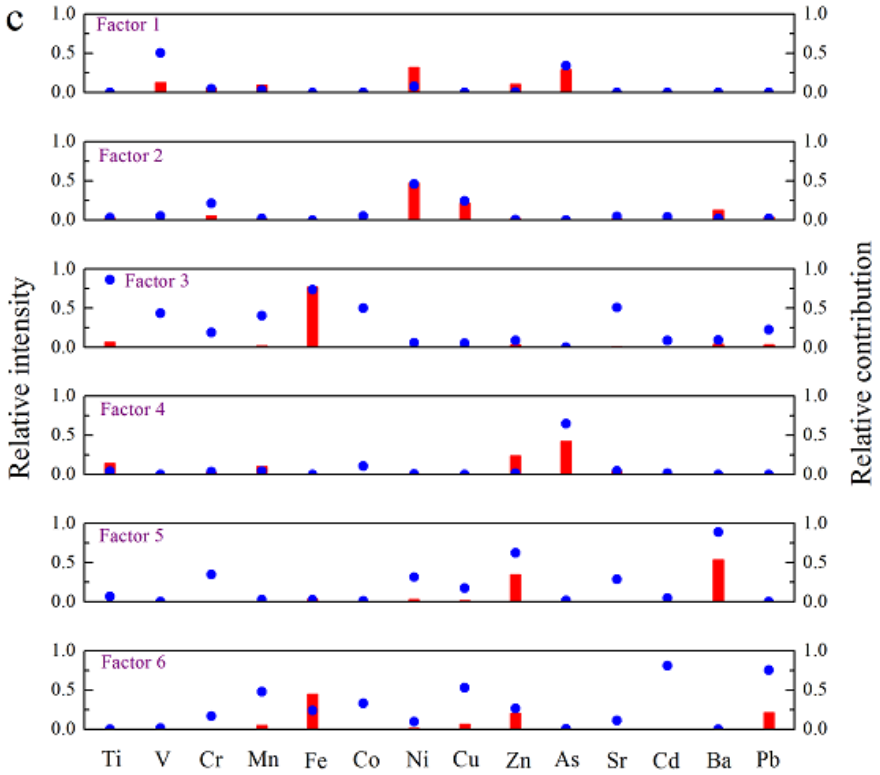

240

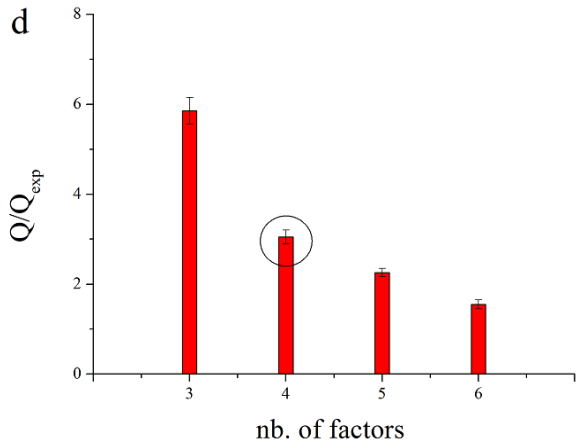

241

242 **Figure S5**. Source profiles resolved from the PMF model with 3 factors (a), 5 factors (b) and
243 6 factors (c), respectively. The bars (left y axis) represent the relative intensity of element to
244 each factor in ng m^{-3}, circles (right y axis) represent the fraction of the total predicted
245 concentration for a given element. The value of goodness-of-fit parameter *Q* (d) corresponded
246 to the source profiles of different number of factors.

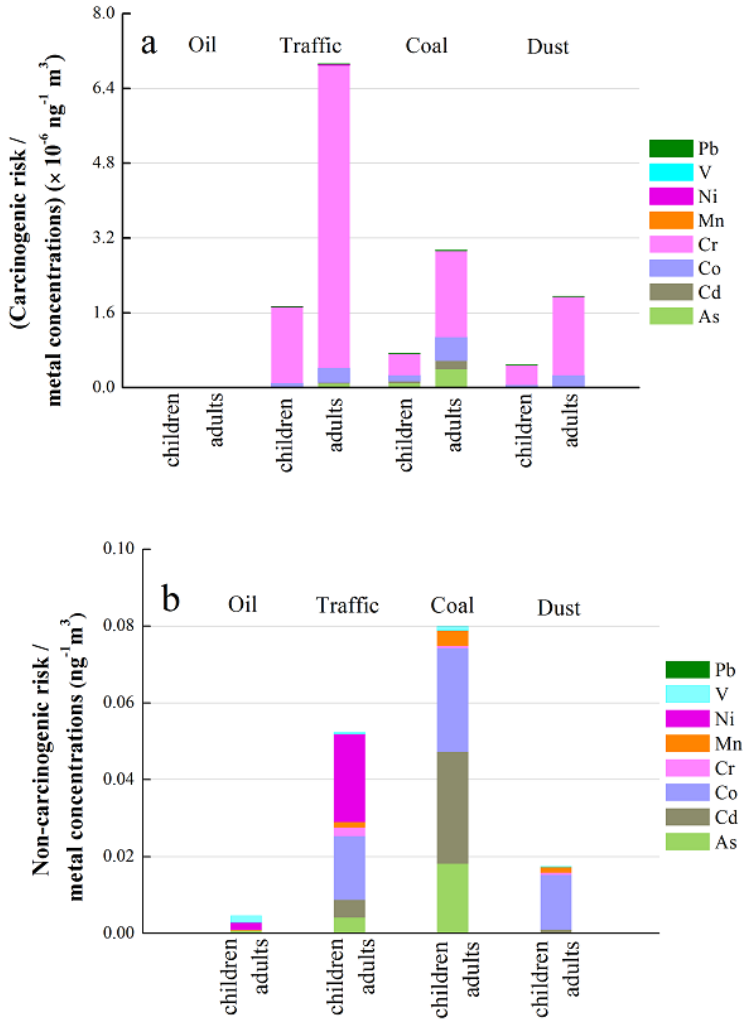

Figure S6. The normalized health risk of toxic elements (As, Cd, Co, Cr (VI), Mn, Ni, V and Pb) in four emission sources.

References

(1) Li, H. M.; Wang, J. H.; Wang, Q. G.; Qian, X.; Qian, Y.; Yang, M.; Li, F. Y.; Lu, H.; Wang, C. Chemical fractionation of arsenic and heavy metals in fine particle matter and its implications for risk assessment: A case study in Nanjing, China. *Atmospheric Environment* **2015**, *103*, 339-346.

(2) Li, H. M.; Wang, Q. G.; Shao, M.; Wang, J. H.; Wang, C.; Sun, Y. X.; Qian, X.; Wu, H. F.; Yang, M.; Li, F. Y. Fractionation of airborne particulate-bound elements in haze-fog episode and associated health risks in a megacity of southeast China. *Environmental Pollution* **2016**, *208*, 655-662.

(3) Polissar, A. V.; Hopke, P. K.; Paatero, P.; Malm, W. C.; Sisler, J. F. Atmospheric aerosol over Alaska: 2. Elemental composition and sources. *Journal of Geophysical Research: Atmospheres* **1998**, *103* (D15), 19045-19057.

(4) Tan, J. H.; Duan, J. C.; Chai, F. H.; He, K. B.; Hao, J. M. Source apportionment of size segregated fine/ultrafine particle by PMF in Beijing. *Atmospheric Research* **2014**, *139*, 90–100.

(5) Volckens, J.; Leith, D. Partitioning theory for respiratory deposition of semivolatile aerosols. *Annals of Occupational Hygiene* **2003**, *47* (2), 157-164.

(6) US EPA (U.S. Environmental Protection Agency), 2009. Risk Assessment Guidance for Superfund (RAGS), Volume I Human Health Evaluation Manual (Part F, Supplemental Guidance for Inhalation Risk Assessment). EPA-540-R-070-002, OSWER 9285.7-82, January. http://www.epa.gov/swerrims/riskassessment/ragsf/index.htm.

(7) US EPA (U.S. Environmental Protection Agency), 2013. User's Guide/technical Background Document for US EPA Region 9's RSL (Regional Screening Levels) Tables. http://www.epa.gov/region9/superfund/prg/.

(8) Taner, S.; Pekey, B.; Pekey, H. Fine particulate matter in the indoor air of barbeque restaurants: elemental compositions, sources and health risks. *Science of the total environment* **2013**, *454-455*, 79-87.

(9) US EPA (U.S. Environmental Protection Agency), 1998. Risk Assessment Guidance for Superfund. In: Human Health Evaluation Manual (Part D), vol. I. https://www.epa.gov/risk/risk-assessment-guidance-superfund-rags-part-d.